Influence of transverse diffusion within the proton beam fast-ignitor scenario

Manuel D. Barriga-Carrasco, Gilles Maynard, and Yuri K. Kurilenkov
Laboratoire de Physique des Gaz et des Plasmas, UMR-8578, Bâtiment 210, Université Paris XI, F-91405 Orsay, France
(Received 13 February 2004; revised manuscript received 2 July 2004; published 22 December 2004)

Fast ignition of an inertial confinement fusion target by an energetic proton beam is here re-examined. We put special emphasis on the role of the transverse dispersion of the beam induced during its travel between the proton source and the compressed deuterium-tritium (DT) fuel. The theoretical model and the computer code used in our calculations are presented. Different beam initial energy distributions are analyzed. We found that the beam exhibits small collective effects while multiple scattering collisions provide a substantial transverse dispersion of the beam. Therefore, the nuclear dispersion imposes severe restrictions on the schemes for fast ignitor even considering an ideal monoenergetic and noncorrelated proton beam.

DOI: 10.1103/PhysRevE.70.066407 PACS number(s): 52.38.Kd, 52.40.Mj, 52.50.Gj, 52.57.Kk

I. INTRODUCTION

We attend in the world to a rapid increase of the number of subpicosecond high intensity laser facilities. In recent years, it has been demonstrated that these lasers can generate, with good efficiency, short bunches of energetic (1–100 MeV) particle beams [1–6]. This rapid development of short-pulse laser beam technology has allowed an alternative approach to inertial confinement fusion (ICF): the fast ignitor (FI) [7].

The fast ignitor concept consists of dissociating the fuel ignition phase from its compression phase. The fuel is previously compressed according to the "traditional" scheme [8] and then it is brought to ignition by means of an external energy source, which should deposit inside the fuel $\approx$10 kJ of energy in less than few picoseconds in order to heat a part of the compressed DT to a temperature above 5 keV. At the final compression phase, the ICF target shows a very sharp density gradient along its radial direction. Its central part has a density up to 1000 times the solid density, whereas the outer part is a low density plasma. A high intensity laser beam focused onto the target will be strongly absorbed at the critical density which, even in highly relativistic regime, is much less than the solid density. Thus the transport of energy from the critical density domain up to the central part of the DT target is one of the main problems for achieving fast ignition of the nuclear fuel.

In the first FI scenario [7] it was suggested that the highly energetic electron beam, generated by the interaction of the laser beam with the target at the relativistic critical density, can propagate up to the compressed DT and then heat it up to the ignition temperature. Several theoretical works and numerical simulations have shown that strong instabilities quickly develop in the early stage of the electron beam propagation, thus reducing to a large extend the amount of energy that can be deposited inside the DT [9]. It has led Roth *et al.* [10] proposed a new scheme in which the electron beam is replaced by a proton one. It has to be noted that the efficiency of energy transport by an electron beam in the first FI scenario is still an open question, in particular concerning the influence of strong density gradient.

In recent experiments [5,6,11] it was demonstrated that proton beams generated by a laser proton source (LPS) have indeed several properties well suited for fast ignition of ICF targets: (i) The energy deposition profile of an energetic proton exhibits a strong peak (the so-called Bragg peak) at the end of the range. Therefore by adjusting the initial proton energy, one can deposit the maximum energy at the required place. (ii) In contradiction to the electron case and due to the large proton mass, the instabilities cannot play a significant role during the beam propagation. (iii) The local emittance of a beam accelerated by a LPS has an extremely low value. That is, all ions coming from a given point of the source have, with a high level of accuracy, the same direction. It is thus possible, by giving the appropriate shape to the source surface to focus the beam to a focal spot with a radius of only a few microns. (iv) The protons are emitted on a short time scale (few picoseconds) compared to the hydrodynamic and diffusion time scale of the target. Thus the LPS can be efficiently used for isochoric heating of dense targets, as it was recently demonstrated [12].

Two important issues of FI with LPS have been recently considered, regarding the influence of the transport between the LPS and the DT on the efficiency of FI. In [13,14] it has been stressed that the distance d_{DT} between the LPS and the DT is limited by the initial energy spread of the proton beam. To induce a large burning ratio of the DT, the proton energy has to be deposited inside the nuclear fuel during the so-called ignition time t_i, during which the density of the central part of the DT keeps its maximum value. The typical value for t_i is 20 ps, while the value of the initial duration of the proton bunch is about $t_{\mathrm{LPS}}=10$ ps. Thus we obtain the relation

$$\frac{\Delta E}{E} \leqslant 2(t_i - t_{\mathrm{LPS}})\frac{V_p}{d_{\mathrm{DT}}} \tag{1}$$

that connects the spread of energy ΔE with d_{DT}, E and V_p being the average energy and velocity of the beam, respectively. Taking $E=15$ MeV and $d_{\mathrm{DT}}=3$ mm (see below) we get $\Delta E \leqslant 5.4$ MeV. The experimental results obtained with present LPS, show that a large part of the beam protons in fact do not satisfy Eq. (1). It has led the authors of [13,14] to recommend placing the LPS closer to the DT that is inside the indirect drive capsule. However, LPS are fast evolving,

new techniques are being considered for reducing the beam initial energy spread [15]. So it seems reasonable to assume that Eq. (1) will be more easily satisfied using the next generation of LPS. A second important issue for the LPS is the influence of collective beam-plasma effects during the protons transport. Numerical results of the transport of a neutralized proton beam in a low density plasma using parameters relevant for FI has been presented in [16]. They show that the critical parameter is the ratio $\xi = n_P/n_B$ between plasma and beam densities. When $\xi < 1$ the beam pinches whereas for $\xi > 1$ the beam propagates almost ballistically, so that collective effects become less important. In case of a density gradient, when the beam encounters a plasma having first $\xi < 1$ and then $\xi \geqslant 1$, the beam diverges quickly because of the transverse velocity acceleration induced during the pinch. The results of [16] have two consequences. First they indicate that the beam should not interfere with a low density plasma and secondly that the LPS should be as large as possible to increase the beam radius and to reduce the initial value of n_B. A beam radius, R_{LPS}, ranging above 100 μm seems to be appropriate.

The work presented here supplements those of [10,13,14,16] by considering the influence of transverse diffusion due to binary collisions, which have not yet been treated. Thus we consider an LPS, which is already optimized with respect to energy spreading and beam-plasma interaction, to determine the remaining main factors that limit the LPS efficiency for fast ignition. Therefore we will first consider an ideal LPS that generates a proton beam, which is optimized to deliver the maximum energy inside the compressed DT target.

As stated before, the FI scenario consists of two consecutive phases. The first one is the compression of the capsule that contains the DT fuel. This compression is obtained on a nanosecond time scale using MJ beams. Both laser and heavy ions beams have been considered for this phase. The crucial point here is to obtain a high level of irradiation uniformity to prevent the growth of hydrodynamic instabilities [9]. A high level of irradiation uniformity can be obtained either by irradiating directly the target by a large number of beams uniformly distributed in the 3D space (the direct drive scenario) or by inserting the DT target inside a blackbody hohlraum (the indirect drive scenario [8]). In the direct drive scenario, it seems difficult to introduce the LPS close to the target without perturbing the homogeneity of the irradiation during the compression phase. Therefore, we will follow the work of [10] and we will consider the proton beam FI within the indirect drive scenario. In order to not interfere with the efficiency of the compression phase, we will first consider that the LPS is put outside the hohlraum capsule. Then our results will concern the same "standard" indirect drive capsule as described in Figs. 1 and 4 of [10]: the diameter of the hohlraum is 5.5 mm, the capsule is made of gold with a thickness of 30 μm and the LPS is placed outside the capsule at a distance of $L = 220$ μm from the gold foil. We will consider the most optimistic situation for the FI: the beam is monoenergetic, the protons energy being $E = 15$ MeV, moreover all protons are focused onto the center of the DT target. The hohlraum plasma is constituted only of low density (10^{17} cm^{-3}) DT plasma. The compressed DT fuel density is 9×10^{25} cm^{-3}, its temperature is 1 keV and its radius is about $R_c = 16$ μm.

The LPS accelerating field is generated by the hot electrons created, through laser-target interaction at high intensity, in the front side of the solid foil. These hot electrons penetrate the foil and by extending past the rear surface produce a strong space-charge field. The acceleration of the target ions during the plasma expansion in the vacuum is similar to ambipolar diffusion in collisionless plasmas, an analysis of this process has been studied for a long time [17–20] (see also references therein). The acceleration process is a rather delicate one. It is highly sensitive to the state of the foil surface and no plasma should be present around the LPS in order to not perturb the acceleration phase. Also the LPS should not be preheated by radiation coming from the capsule, otherwise the hydrogen atoms will be desorbed from the target, generating a density gradient that will greatly affect the acceleration mechanism. The capsule wall in front of the LPS should absorb the x-ray radiation coming from the hohlraum, which has a temperature of more than 200 eV during several nanoseconds. Moreover the inner part of the wall has to be made of high-Z material, otherwise it will expand quickly and interact with the target containing the DT during the compression phase. Therefore, our first consideration is to place a rather thick gold foil in front of the LPS. Its thickness is 30 μm, which is the standard value for the indirect drive capsule. We show below that this foil induces a too large transverse dispersion. Then we analyze the dependence of the transverse dispersion with the beam energy distribution and with the position and thickness of the protecting gold foil.

In previous works [10,13,14], the FI scenario with protons was investigated without considering transverse dispersion of the beam. This assumption is generally valid when describing the transport of beam ions generated by standard accelerators for which the transverse beam size is of the order of millimeters. However, in the case of an LPS, and more particularly for FI application, the transverse dimension of both the source and the target is so small that even a small transverse dispersion can greatly affect the density of the deposited energy inside the target. In [16] it is shown that collective beam-plasma effects can lead to a large transverse dispersion. Here we consider that the surface of the source is large enough so that the beam will encounter only overdense plasma ($\xi > 1$) in which collective beam-plasma effects are greatly reduced. In any case, the collective effects will mainly add an additional transverse dispersion to the microscopic collisions. So the value of transverse dispersion that we obtain can be considered as the minimum one within the considered configuration.

Our theoretical model is detailed in Sec. II, then we present the basic ingredients of our numerical code MBC-ITFIP (Sec. III), whose results within the fast ignitor scenario are analyzed in Sec. IV.

II. THEORETICAL MODEL

A. Electronic collisions

We can distinguish two different kinds of collisions with the target material: the interaction with the target electronic

medium and the interaction with the target nuclei. At energies >1 MeV the electronic stopping dominates over the nuclear one, whereas nuclear interactions are the main cause of the projectile angular dispersion [21].

For protons with $E>1$ MeV, the perturbation parameter $\eta=v_B/V_p$, where $v_B=2.19\times10^8$ cm/s is the Bohr velocity, is much smaller than one. So the electronic stopping force can be determined using the first order quantum approximation. We take into account collective effects of plasma electrons through the dielectric formalism [22,23]. Thus the stopping force acting on the proton is then given by

$$S_{\mathrm{p0}}=\frac{e^2}{\epsilon_0(2\pi)^3V_p}\int d^3q\frac{\mathbf{q}\cdot\mathbf{V}_p}{q^2}\,\mathrm{Im}\left[\frac{-1}{\epsilon(q,\mathbf{q}\cdot\mathbf{V}_p)}\right] \tag{2}$$

and the energy loss straggling per unit path length is

$$\Omega^2=\frac{e^2}{\epsilon_0(2\pi)^3V_p}\int d^3q\frac{(\mathbf{q}\cdot\mathbf{V}_p)^2}{q^2}\,\mathrm{Im}\left[\frac{-1}{\epsilon(q,\mathbf{q}\cdot\mathbf{V}_p)}\right]. \tag{3}$$

The target electron fluid is characterized by its energy loss function, $\mathrm{Im}[-1/\epsilon(q,\mathbf{q}\cdot\mathbf{V}_p)]$, which contains relevant information about its response to electronic excitations with momentum q induced by the passage of the swift charge.

A direct evaluation of Eqs. (2) and (3) within the numerical simulation of the proton transport process will require an excessive amount of computer resources. To solve this problem, we use analytical formulas in the limit of low and high projectile velocities from which an interpolating expression is derived for intermediate velocities.

Let us consider a target with an atomic number Z_n and an atomic density $\mathcal{N}$. Using the average atom model [24], we can determine the mean ionization Q, the free electron density $n=Q\mathcal{N}$ and the bound electron density for each shell $n_i=P_i\mathcal{N}$, where P_i is the number of electrons in the i shell of the average atom. Then Eq. (2) is put in the form

$$S_{\mathrm{p0}}=\frac{e^4\mathcal{N}}{4\pi\epsilon_0^2m_eV_p^2}L_e, \tag{4}$$

m_e being the electron mass. The stopping number L_e is defined as

$$L_e=QL_F+\sum_i P_iL_i, \tag{5}$$

where L_F is the stopping number for free electrons and L_i is the stopping number for bound electrons. We calculated each L_x by interpolating between the asymptotic formulas valid either for low or for high projectile velocities compared to the average electron velocity [25]:

$$L_x(V_p)=\begin{cases}L_{\mathrm{H}}(V_p)=\ln\left(\dfrac{2m_eV_p^2}{\overline{I}}\right)-\dfrac{2K}{m_eV_p^2} & \text{for } V_p>V_{\mathrm{int}},\\[2ex] L_{\mathrm{B}}(V_p)=\dfrac{\alpha V_p^3}{1+GV_p^2} & \text{for } V_p\leqslant V_{\mathrm{int}},\end{cases} \tag{6}$$

$$V_{\mathrm{int}}=\sqrt{\frac{3K+1.5\overline{I}}{m_e}}, \tag{7}$$

where G is given by $L_{\mathrm{H}}(V_{\mathrm{int}})=L_{\mathrm{B}}(V_{\mathrm{int}})$, K is the electron kinetic energy, $\overline{I}$ is the mean excitation potential and α is the friction coefficient at low velocities.

For free electrons $\overline{I}=\hbar\omega_p=\hbar\sqrt{ne^2/(\epsilon_0m_e)}$, ω_p being the plasma frequency; $K\simeq k_BT+E_{\mathrm{F}}$, where $E_{\mathrm{F}}=0.5(3\pi^2n)^{2/3}\hbar^2/m_e$ is the Fermi energy, T is the target temperature, k_B is the Boltzmann constant and α is determined from Fermi functions [25]. For bound electrons $\overline{I}=\sqrt{2Ka_B^2/(E_B\langle r^2\rangle)}$, where $E_B=27.2$ eV and $a_B=0.53\times10^{-8}$ cm are the atomic units of energy and length, respectively. The kinetic energy K and the average of the square of the radial position $\langle r^2\rangle$ for each shell are determined by solving the Schrödinger equation within the average atom. The friction coefficient for the bound electrons is found using the impulse approximation, yielding $\alpha=1.067E_B^{3/2}\sqrt{K}/(\overline{I}^2v_B^2)$ [26].

In the same way, the electronic straggling is written as

$$\Omega^2=\frac{e^4\mathcal{N}}{4\pi\epsilon_0^2m_eV_p^2}L_{\Omega e}, \tag{8}$$

with

$$L_{\Omega e}=QL_{\Omega F}+\sum_i P_iL_{\Omega i}. \tag{9}$$

Each $L_{\Omega x}$ has the form

$$L_{\Omega x}(V_p)=\begin{cases}L_{\Omega\mathrm{H}}(V_p)=m_eV_p^2+\dfrac{2K}{3}\ln\left(\dfrac{2m_eV_p^2}{\overline{I}_1}\right) & \text{for } V_p>V_{\mathrm{int}},\\[2ex] L_{\Omega\mathrm{B}}(V_p)=\dfrac{\alpha_\Omega V_p^3}{1+G_\Omega V_p^2} & \text{for } V_p\leqslant V_{\mathrm{int}},\end{cases} \tag{10}$$

where G_Ω is given by $L_{\Omega\mathrm{H}}(V_{\mathrm{int}})=L_{\Omega\mathrm{B}}(V_{\mathrm{int}})$ and

$$\alpha_\Omega=\alpha\overline{I}\ln\left(1+\frac{2V_p\sqrt{2Km_e}}{\overline{I}}\right). \tag{11}$$

For free electrons $\overline{I}_1=\overline{I}$, defined before, and for bound electrons

$$\overline{I}_1=\frac{4K}{3}\frac{(\ell+3/2)}{\sqrt{(\ell+5/2)(\ell+1/2)}}, \tag{12}$$

where ℓ is the orbital quantum number of the electronic level.

B. Nuclear collisions

Nuclear interactions are treated within the classical dispersion theory. In the center of mass frame, the angle $\theta(s)$ with which a proton with energy E and impact parameter s is scattered from a target nucleus with atomic number Z_n and mass M_n is given by [27]

$$\theta(s) = \pi - 2s\int_{R_{\min}}^{\infty} \frac{dr}{r^2\sqrt{1 - V(r)/E_r - s^2/r^2}}, \qquad (13)$$

where $E_r = 4M_pM_nE/(M_p+M_n)^2$ is the maximum transferable energy, and $R_{\min}$ is the distance of minimum approach. The potential energy $V(r)$ is written as

$$V(r) = \frac{Z_n e^2}{4\pi\varepsilon_0 r}\Phi\left(\frac{r}{a}\right). \qquad (14)$$

For a cold target, Φ is the Thomas-Fermi screening function and a is the universal screening length [21]:

$$a = 0.8854a_B/(1 + Z_n^{0.23}). \qquad (15)$$

For a fully ionized plasma Φ is the Debye potential $\Phi(r/a) = \exp(-r/a)$ and a is the dynamical adiabatic screening length, which depends on temperature:

$$a = (\sqrt{v_{th}^2 + V_p^2})/\omega_p,$$

where $v_{th} = \sqrt{2k_BT/m_e}$ is the plasma thermal velocity. For a partially ionized plasma, Φ and a are obtained from the average atom model [24].

The elastic collision induces an energy E_T transferred to the nucleus, and therefore lost by the projectile. It is related to the scattering angle θ by

$$E_T = \frac{4M_pM_nE}{(M_p + M_n)^2}\sin^2(\theta/2), \qquad (16)$$

so the greater the scattering angle, the greater the energy loss. In our energy regime, Eq. (16) introduces only a small correction to the inelastic proton energy loss, Eq. (2).

The presented theoretical model has been implemented in our simulation code. This code describes the propagation of independent ions, given their initial energy and radial distributions.

III. NUMERICAL CODE

We have constructed a simulation code, named MBC-ITFIP, to follow the trajectories of energetic light ions interacting with dense plasmas. This code is derived from a previous one which had been used and checked for cold targets [28–30]. Here it is summed up in a few main points related with the present work.

The simulation code uses a standard 3D molecular dynamics method to follow the evolution of the protons. The electronic stopping force S_p, acting on a proton during a time step Δt is obtained from a draw of a Gaussian distribution whose mean value is the electronic stopping S_{p0}, Eq. (4), and with a variance $\Omega^2/\Delta z$, where Ω^2 is the electronic straggling, Eq. (8), and $\Delta z = V_p\Delta t$:

$$\mathcal{P}_{\text{stop}}(S_p) = \frac{1}{\sqrt{2\pi}\sqrt{\Omega^2/\Delta z}}\exp\left[-\frac{1}{2}\frac{(S_p - S_{p0})^2}{\Omega^2/\Delta z}\right]. \qquad (17)$$

The method used for the nuclear scattering is based on the binary collision model described by Möller *et al.* [31] and on the Monte Carlo simulation method developed by Zajfman *et al.* [32]. In our code, only rare events corresponding to large scattering angles, $\theta' \geqslant \theta_c$, will be considered in the Monte Carlo draw and multiple scattering small angles, $\theta' \leqslant \theta_c$, will be treated as a continuum process. Large and small scattering angle events are also called hard and soft collisions, respectively. To take into account the effects of the multiple soft collisions along the distance to the next hard collision, we use the same method as for the electronic force. The resulting angle θ is obtained from a draw of a Gaussian distribution whose mean value is the hard collision angle, θ_h (selected by the Monte Carlo method), and whose variance is the straggling due to soft collisions

$$\mathcal{P}_n(\theta) = \frac{1}{\sqrt{2\pi}\sqrt{\langle\theta^2\rangle_s}}\exp\left[-\frac{1}{2}\frac{(\theta - \theta_h)^2}{\langle\theta^2\rangle_s}\right], \qquad (18)$$

where

$$\langle\theta^2\rangle_s = \mathcal{N}d_h\int_0^{\theta_c}\theta'^2\frac{d\sigma}{d\theta}d\theta', \qquad (19)$$

d_h being the distance between the considered two hard collisions. The proton energy lost in the elastic collision is given by Eq. (16). This method for nuclear scattering improves computer simulation time more than 10^3 times, compared to the full Monte Carlo method.

IV. RESULTS

In this section we apply the MBC-ITFIP code to study the beam radial distribution and energy deposition in the compressed fuel for the FI scenario described in Sec. I.

First we consider an ideal monoenergetic proton beam without initial angular dispersion, which is focused onto the DT target. The initial beam energy is 15 MeV for which there is a maximum energy deposition in the compressed fuel for the specified FI scenario. Figure 1(a) represents the proton distribution arriving to the core in the *xy* plan perpendicular to the beam propagation axis *z*. The energy deposition profile in the compressed fuel is represented in Fig. 1(b) along *z* and *y* directions. From Fig. 1(b) we conclude, in accordance with previous works [10,13,14], that the beam spread in the longitudinal direction induced by the straggling in the energy loss is compatible with the FI, as the ions arriving to the DT fuel are stopped in the first few μm. However, the main feature exhibits by Fig. 1 is that *most part of the incoming protons does not interact with the compressed DT fuel*. The mean beam radius at the core is in fact much greater than the core radius. The deposited energy is therefore mostly outside the compressed fuel. The standard deviation of the beam radial distribution is found to be about $\sigma_\rho = 80$ μm whereas the radius of the core is 16 μm. In this situation, *less than 1% of the beam energy is used to heat the fuel*. Therefore we can conclude that the efficiency as an FI of an LPS placed outside a standard capsule is greatly reduced by the large angular diffusion induced by the interaction with the protecting gold foil. Moreover, this conclusion remains valid even with an ideal monoenergetic beam with zero emittance. Therefore, either a specific window has to be put in front of the LPS or, the protecting gold foil has to be closer to the DT target.

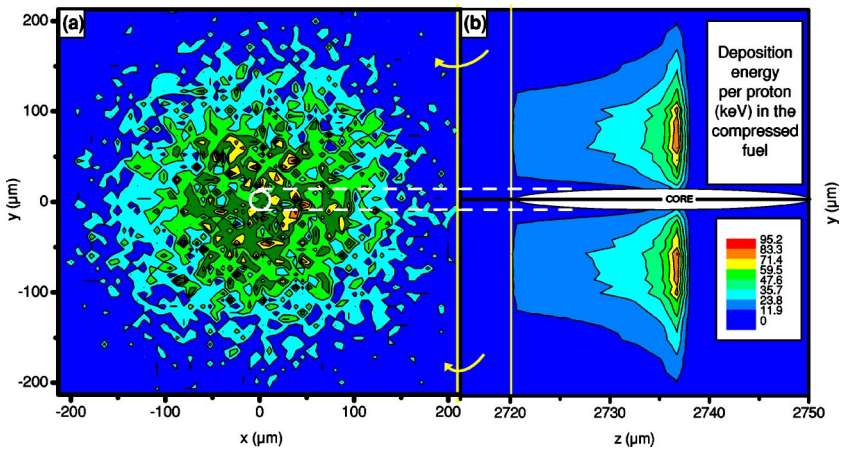

FIG. 1. (Color online) (a) 15 MeV proton beam perpendicular distribution and (b) proton energy deposition in the core (z =2720 μm).

To get a better insight on the influence of the relevant parameters, we have determined the evolution of the transverse dispersion of the beam with some factors related with the specific FI scenario. Figure 2(a) shows the radial distribution (ρ distribution) of the 15 MeV protons for the same case as in Fig. 1, but varying the gold wall thickness (δ) from 3 to 30 μm. As we can see, the width of the ρ distribution becomes similar to the radius of the compressed fuel only for the thinnest thickness.

The evolution of the transverse dispersion with the distance D between the protecting gold foil and the center of the DT target is reported in Fig. 2(b) for a gold foil thickness δ=30 μm. We see in this figure, that the part of the protons that does not penetrate the compressed fuel becomes negligible only below the smallest considered distance of 70 μm. It indicates that it is better to reduce distance D than the gold foil thickness. Finally, we have reported in Fig. 3 the evolution of the standard deviation, σ_ρ, of the ρ distribution with

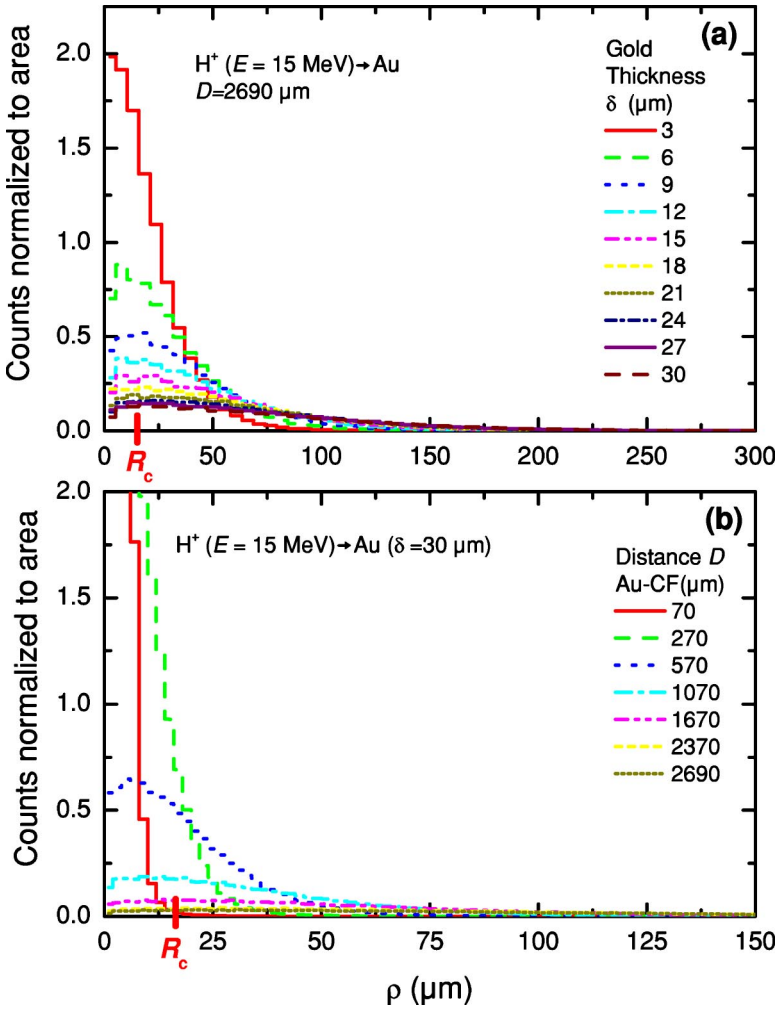

FIG. 2. (Color online) ρ (perpendicular) distribution of 15 MeV protons arriving to compressed fuel (a) at D=2690 μm and for different gold thicknesses, δ, (b) at different D distances and for δ=30 μm.

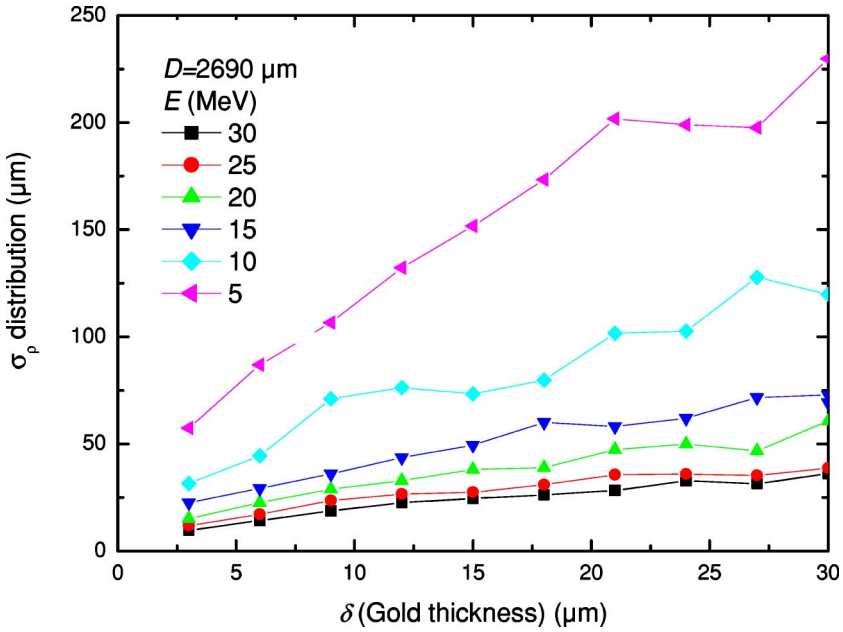

FIG. 3. (Color online) σ_ρ as a function of gold foil thickness for protons of different energies, E, arriving to compressed fuel at $D=2690$ μm.

the proton energy E. As we can see, σ_ρ depends almost inversely on the proton energy. The initial distribution of energy is fixed by the condition that the Bragg peak should be located within the compressed DT, so the maximum of the proton energy cannot be much larger than 15 MeV. The results reported in Fig. 3 indicate that a broadening of the energy distribution toward lower energy will lead to a reduction of the efficiency of FI due to a larger transverse dispersion.

We can sum up all former results in just one formula:

$$\sigma_\rho(\mu\mathrm{m}) \approx 0.07 \frac{\sqrt{\delta(\mu\mathrm{m})}(D+\delta)(\mu\mathrm{m})}{E(\mathrm{MeV}) - 0.15\delta(\mu\mathrm{m})/E(\mathrm{MeV})}. \quad (20)$$

This relation is valid for $E \geqslant 5$ MeV and for a reasonable value of δ, so that the energy lost within the gold foil remains small compared to the initial energy. Equation (20) indicates the transverse dispersion at the target center due to the interaction of the beam with the gold wall. The additional transverse dispersion induced by the plasma around the core gives only a small contribution compared to the gold one because it is made of light material. We retrieve in this equation that $\langle\theta^2\rangle_s$ increases linearly with the number of collisions, Eq. (19), i.e., with the wall thickness (δ), and that σ_ρ increases with the distance from the gold foil to the target center (D), as $\rho=(D+\delta)\tan(\theta)$.

From Eq. (20), we can estimate the value of D where the protecting foil has to be situated in order for most protons to penetrate in the core radius, i.e., $\sigma_\rho < 16$ μm, keeping the other parameters unchanged. For $E=15$ MeV and $\delta=30$ μm, we get $D<500$ μm, so the LPS window should not to be placed far away from the compressed fuel core. In [14] it was found, neglecting the transverse diffusion, that due to the energy distribution of the present LPS, the capsule must have a specific design, in which the LPS can be put close to the DT. Here we conclude that also the protecting gold foil should be placed closer to the DT because of the beam transverse dispersion in this foil. This statement remains true even in the case of a substantial improvement of the beams generated by LPS.

To get a realistic result according to present technologies, we have analyzed the influence of the initial energy spread of the beam to the transverse diffusion using a distribution observed in recent experiments [33], which is reported in Fig. 4. Our results, using the values of Fig. 4 and situating the protecting foil at the maximum recommended distance from the DT ($D \approx 500$ μm), are reported in Figs. 5. In Fig. 5(a) we observe that the final proton radial distribution width at the core is larger than the value obtained for a 15 MeV monoenergetic beam with the protecting foil at the same distance from the DT. This is because the average value of the proton energy distribution is lower than 15 MeV and, as σ_ρ is al-

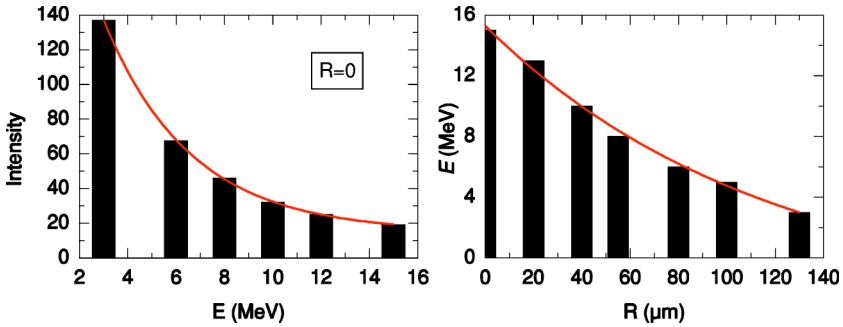

FIG. 4. (Color online) Typical example of the energy distributions of a proton beam with radius R generated by a LPS created by the 30 J, 300 fs pulse of the 100 TW laser, at LULI, Palaiseau, France [33].

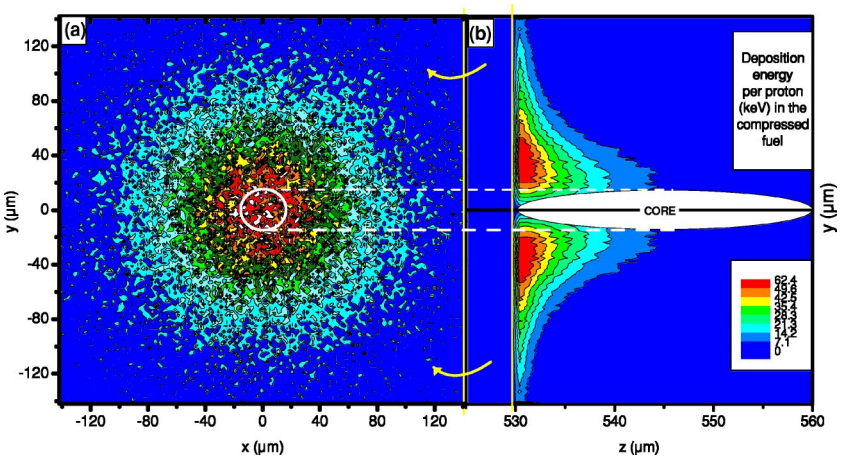

FIG. 5. (Color online) Results obtained with the energy distribution of Fig. 4: (a) perpendicular distribution of the beam and (b) proton energy deposition in the core ($z=530$ μm).

most inversely proportional to the proton energy, Eq. (20), the transverse diffusion of this beam is larger. In Fig. 5(b) we have reported the energy deposition in the core along z and y directions for the initial beam energy distribution from Fig. 4. Obviously, we observe a larger transverse spreading for the density of the deposited energy than the calculated for a monoenergetic beam, since the beam energy distribution introduces an additional increasing of the beam transverse dispersion due to the LPS protecting wall.

As stated in the Introduction, putting the LPS outside the capsule has the great advantage of not perturbing the compression phase inside the capsule. Therefore, it is important to determine the configuration which can provide an efficient protection of the LPS together with a low transverse dispersion of the proton beam. The parameters to be determined are the distances between the LPS and the protecting foil (L), and between the foil and the DT core (D), and also the thickness (δ) and the composition of the foil. A detailed analysis of this configuration will require an investigation of the transport of heat and plasma between the capsule and the LPS, and also of the types of perturbation that are acceptable for the LPS without reducing significantly its efficiency. Here we present a preliminary analysis of this problem, using the MULTI code of Ramis *et al.* [34], and considering the protecting gold foil thickness (δ) as the only parameter to be optimized.

For the LPS to be able to produce a high quality proton beam at high energy, it must be operated within specific conditions. In particular, the rear surface of the LPS, which is in front of the capsule, should not be preheated by radiation or polluted by a plasma coming from the capsule. Moreover, it has been shown that the efficiency of the proton acceleration mechanism is highly sensitive to an ion density gradient at the rear surface [6].

Using the MULTI code, we have investigated the evolution of a gold foil, whose inner side is irradiated by the hohlraum black-body radiation. For the evolution of the hohlraum radiation temperature with time, we have considered a National Ignition Facility (NIF) type target, the values of which being given in the MULTI package. This evolution is reported in Fig. 6. We see in this figure that the ignition time, that is the time at which the LPS should operate, is 17.5 ns. First we have a 8 ns prepulse of $\approx$80 eV, then the temperature reaches 150 eV during 3 ns, and finally the main pulse yields a radiation temperature of 300 eV inside the hohlraum during 2 ns. When considering a 30 μm thick gold foil, we observed that only the first prepulse has enough time to propagate up to the outer wall of the foil. In this case the temperature of the external surface of the gold foil is about 10 eV. Thus, even for a 30 μm thickness, the LPS should not be put too close to the capsule wall. Furthermore, during the 17.5 ns of irradiation, the inner gold wall expands up to 1.3 mm inside the capsule. Thus the radius of the protecting window R_W in front of the LPS should be about 1 mm larger than the radius of the beam, R_{LPS}.

We have seen that a reasonable value of the transverse dispersion is obtained for a gold thickness of less than 3 μm. At this thickness value, the shock wave induced by the main pulse arrives at the outer surface of the gold foil well before the ignition time. The evolution of the temperature at the outer surface of the gold foil is reported on Fig. 6. We see in this figure that during the last 3 ns before the ignition time, the temperature is above 100 eV.

To estimate the distance L at which the LPS should be put from the gold foil, a 100 μm thick carbon foil has been

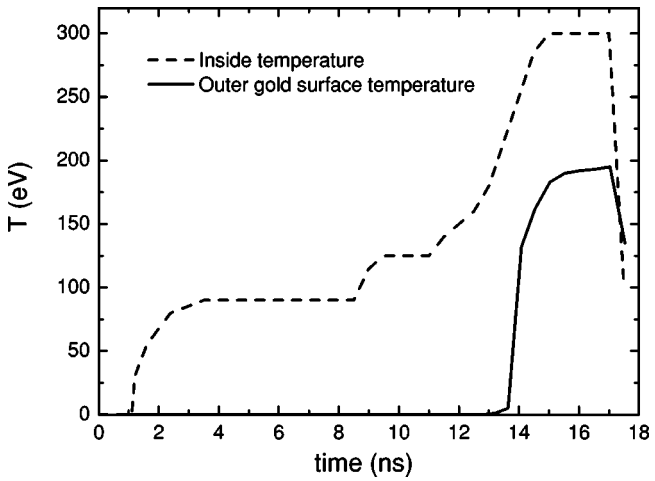

FIG. 6. Temperature evolution time for a NIF-type indirect driven target. Dashed line: radiation temperature inside the hohlraum; solid line: radiation temperature from the outer wall of a 3 μm thick gold foil, calculated by the MULTI code [34].

irradiated by a thermal radiation, whose temperature is equal to the capsule's outer surface one. The thermal flux at the carbon foil has been reduced by a factor F to simulate the decrease with L of the thermal flux interacting with the LPS. Our calculations showed that the temperature of the carbon surface at the ignition time is smaller than 1 eV only when F becomes less than 10^{-4}. The radiation flux at the LPS decreases as $[1-\cos(\theta)]$ with $\tan(\theta)=R_W/L$, taking $R_W=1$ mm, we get $L \geqslant 7$ cm. Using Eq. (1), this value of L requires an energy spread ΔE less than 0.25 MeV, which seems quite demanding. The obtained numbers should not be considered as definitive values. In particular R_W at the outer surface, will depend on the actual value of R_{LPS}, which in turn depends on the LPS efficiency and also on the importance of the transverse dispersion during the transport. Nevertheless, the above analysis demonstrates that transverse dispersion induced by multi-scattering collisions imposes severe constraints that should be considered to design a realistic configuration for fast ignition by a proton beam.

V. CONCLUSIONS

The main conclusion of this work is that realistic applications of energetic proton beams generated by high flux laser irradiation cannot be investigated without taking into account the angular dispersion of the beam. In more conventional accelerators, the emittance of the beam is in the range of mm.mrad so that the angular diffusion is generally not an important process. However laser proton sources generate beams with an emittance several orders of magnitude smaller than in conventional accelerators. To take full advantage of this low emittance for depositing more than 10 MJ/g in a DT target, it is necessary that the transverse dispersion remains at a very small value during the transport of the proton beam. Concerning the influence of multi-scattering, the main technical problem seems to be protecting efficiently the laser source, without introducing a large amount of heavy elements in the path of the proton. The largest distance between the protecting gold foil and the DT can be determined from Eq. (20).

More generally, when investigating the interaction of an energetic beam generated by an LPS with a dense target, the longitudinal dispersion will be mainly due to the energy distribution of the source while the transverse dispersion will reveal the statistical distribution of the microscopic microfield fluctuation inside the target. The LPS source can then be used as a very sensitive probe of microfields inside a dense plasma provided the analysis is sustained by an accurate theoretical modeling of the interaction process. This is the aim of the model we have presented in this paper, which through the use of simple analytical formula can be easily implemented in a simulation code to analyze quantitatively experimental situations.

ACKNOWLEDGMENTS

This work was financed by CEA-EURATOM (under Project No. V.3094.003). M.D.B-C. thanks Fundación Séneca for financial support.

[1] V. Malka, S. Fritzler, E. Lefebvre, M.-M. Aleonard, F. Burgy, J.-P. Chambaret, J.-F. Chemin, K. Krushelnick, G. Malka, S. P. D. Mangles, Z. Najmudin, M. Pittman, J.-P. Rousseau, J.-N. Scheurer, B. Walton, and A. E. Dangor, Science **298**, 1596 (2002).

[2] M. Hegelich, S. Karsch, G. Pretzler, D. Habs, K. Witte, W. Guenther, M. Allen, A. Blazevic, J. Fuchs, J. C. Gauthier, M. Geissel, P. Audebert, T. Cowan, and M. Roth, Phys. Rev. Lett. **89**, 085002 (2002).

[3] E. L. Clark, K. Krushelnick, J. R. Davies, M. Zepf, M. Tatarakis, F. N. Beg, A. Machacek, P. A. Norreys, M. I. K. Santala, I. Watts, and A. E. Dangor, Phys. Rev. Lett. **84**, 670 (2000).

[4] R. Kodama, K. A. Tanaka, Y. Sentoku, T. Matsushita, K. Takahashi, H. Fujita, Y. Kitagawa, Y. Kato, T. Yamanaka, and K. Mima, Phys. Rev. Lett. **84**, 674 (2000).

[5] R. A. Snavely, M. H. Key, S. P. Hatchett, T. E. Cowan, M. Roth, T. W. Phillips, M. A. Stoyer, E. A. Henry, T. C. Sangster, M. S. Singh, S. C. Wilks, A. MacKinnon, A. Offenberger, D. M. Pennington, K. Yasuike, A. B. Langdon, B. F. Lasinski, J. Johnson, M. D. Perry, and E. M. Campbell, Phys. Rev. Lett. **85**, 2945 (2000).

[6] M. Roth, A. Blazevic, M. Geissel, T. Schlegel, T. E. Cowan, M. Allen, J.-C. Gauthier, P. Audebert, J. Fuchs, J. Meyer-ter-Vehn, M. Hegelich, S. Karsch, and A. Pukhov, Phys. Rev. ST Accel. Beams **5**, 061301 (2002).

[7] M. Tabak, J. Hammer, M. E. Glinsky, W. L. Kruer, S. C. Wilks, J. Woodworth, E. M. Campbell, M. D. Perry, and R. J. Mason, Phys. Plasmas **1**, 1626 (1994).

[8] J. Lindl, Phys. Plasmas **2**, 3933 (1995).

[9] C. Deutsch, Eur. Phys. J.: Appl. Phys. **24**, 95 (2003).

[10] M. Roth, T. E. Cowan, M. H. Key, S. P. Hatchett, C. Brown, W. Fountain, J. Johnson, D. M. Pennington, R. A. Snavely, S. C. Wilks, K. Yasuike, H. Ruhl, F. Pegoraro, S. V. Bulanov, E. M. Campbell, M. D. Perry, and H. Powell, Phys. Rev. Lett. **86**, 436 (2001).

[11] T. E. Cowan, J. Fuchs, H. Ruhl, A. Kemp, P. Audebert, M. Roth, R. Stephens, I. Barton, A. Blazevic, E. Brambrink, J. Cobble, J. Fernández, J.-C. Gauthier, M. Geissel, M. Hegelich, J. Kaae, S. Karsch, G. P. Le Sage, S. Letzring, M. Manclossi, S. Meyroneinc, A. Newkirk, H. Pépin, and N. Renard-LeGalloudec, Phys. Rev. Lett. **92**, 204801 (2004).

[12] P. K. Patel, A. J. Mackinnon, M. H. Key, T. E. Cowan, M. E. Foord, M. Allen, D. F. Price, H. Ruhl, P. T. Springer, and R. Stephens, Phys. Rev. Lett. **91**, 125004 (2003).

[13] S. Atzeni, M. Temporal, and J. J. Honrubia, Nucl. Fusion **42**, L1 (2002).

[14] M. Temporal, J. J. Honrubia, and S. Atzeni, Phys. Plasmas **9**, 3098 (2002).

[15] T. Zh. Esirkepov, S. V. Bulanov, K. Nishihara, T. Tajima, F. Pegoraro, V. S. Khoroshkov, K. Mima, H. Daido, Y. Kato, Y.

Kitagawa, K. Nagai, and S. Sakabe, Phys. Rev. Lett. **89**, 175003 (2002).
[16] H. Ruhl, T. Cowan, J. Dhlburg, P. Parks, and R. Stephens, Nucl. Fusion **44**, 438 (2004).
[17] J. Denavit, Phys. Fluids **22**, 1384 (1979).
[18] S. C. Wilks, A. B. Langdon, T. E. Cowan, M. Roth, M. Singh, S. Hatchett, M. H. Key, D. Pennington, A. MacKinnon, and R. A. Snavely, Phys. Plasmas **8**, 542 (2001).
[19] P. Mora, Phys. Rev. Lett. **90**, 185002 (2003).
[20] K. Matsukado, T. Esirkepov, K. Kinoshita, H. Daido, T. Utsumi, Z. Li, A. Fukumi, Y. Hayashi, S. Orimo, M. Nishiuchi, S. V. Bulanov, T. Tajima, A. Noda, Y. Iwashita, T. Shirai, T. Takeuchi, S. Nakamura, A. Yamazaki, M. Ikegami, T. Mihara, A. Morita, M. Uesaka, K. Yoshii, T. Watanabe, T. Hosokai, A. Zhidkov, A. Ogata, Y. Wada, and T. Kubota, Phys. Rev. Lett. **91**, 215001 (2003).
[21] M. Nastasi, J. W. Mayer, and J. K. Hirvonen, *Ion-Solid Interactions* (Cambridge University Press, Cambridge, England, 1996).
[22] J. Lindhard, K. Dan. Vidensk. Selsk. Mat. Fys. Medd. **28**, 8 (1954).
[23] J. Lindhard and A. Winther, K. Dan. Vidensk. Selsk. Mat. Fys. Medd. **34**, 8 (1963).
[24] G. Maynard, C. Deutsch, K. Dimitriou, K. Katsonis, and M. Sarrazin, Nucl. Instrum. Methods Phys. Res. B **195**, 188 (2002).
[25] G. Maynard and C. Deutsch, J. Phys. (France) **46**, 1113 (1985).
[26] X. Garbet, C. Deutsch, and G. Maynard, J. Appl. Phys. **61**, 907 (1987).
[27] H. Goldstein, *Classical Mechanics* (Addison-Wesley, Reading, MA, 1980).
[28] R. Garcia-Molina, C. D. Denton, I. Abril, and N. R. Arista, Phys. Rev. A **62**, 012901 (2000).
[29] R. Garcia-Molina and M. D. Barriga-Carrasco, Phys. Rev. A **68**, 054901 (2003).
[30] M. D. Barriga-Carrasco and R. Garcia-Molina, Phys. Rev. A **68**, 062902 (2003).
[31] W. Möller, G. Pospiech, and G. Schrieder, Nucl. Instrum. Methods **130**, 265 (1975).
[32] D. Zajfman, G. Both, E. P. Kanter, and Z. Vager, Phys. Rev. A **41**, 2482 (1990).
[33] P. Audebert (private communication).
[34] R. Ramis, R. Schmaltz, and J. Meyer-ter-Vehn, Comput. Phys. Commun. **49**, 475 (1988); http://server.faia.upm.es/multi